



# Calculation of phase transformation latent heat based on cooling curves in end-quench test and its application in nickel-based superalloy

Tian-yang ZHAO<sup>1</sup>, Pei FU<sup>1</sup>, Zhuo CHEN<sup>1</sup>, Ping ZHOU<sup>1</sup>, Chao LI<sup>2</sup>

1. School of Energy Science and Engineering, Central South University, Changsha 410083, China;

2. State Key Laboratory of Powder Metallurgy, Central South University, Changsha 410083, China

Received 9 May 2021; accepted 26 October 2021

**Abstract:** To obtain the phase transformation latent heat corresponding to different cooling rates with low test workload and cost, the Newton thermal analysis method and the improved Newtonian thermal analysis method were discussed based on the cooling curve obtained in the end-quench test. The validity of two methods was given by the latent heat calculation of 45<sup>#</sup> steel. The results show that the relative error of latent heat is 5.20% through the improved Newtonian thermal analysis method, which is more accurate than the Newtonian thermal analysis method. Furthermore, the latent heat release of phase transformation of the self-designed CSU-A1 powder metallurgy nickel-based superalloy increases from 4.3 to 12.29 J/g when the cooling rate decreases from 50.15 to 33.40 °C/min, because there is more sufficient time for the alloy microstructure to complete the phase transformation process when the cooling rate is smaller.

**Key words:** cooling curve; end-quench test; Newtonian thermal analysis method; phase transformation latent heat; nickel-based superalloy

## 1 Introduction

To study the relationship between the cooling rate, and the microstructure and mechanical properties, the end-quench test is proposed as a high-throughput way with high efficiency and low cost [1–3]. The phase transformation of alloy, which happens when the microstructural phase equilibrium is broken due to the temperature changing, is important to affect the temperature field and the cooling rate during the cooling process.

During the phase transformation process, the microstructure changes from the unstable high energy state to the low energy state, such as changes in crystal structure, chemical composition, and degree of order. Thus, the latent heat is released due to the different thermophysical parameters of

different phases. The latent heat is considered to be proportional to the fraction of the solidified alloy, which is affected by many factors, such as the cooling rate, the phase transformation temperature and the phase transformation time [4].

Based on the experiment, thermal analysis method, microstructure analysis method (such as synchrotron diffraction techniques, transmission and scanning electron microscopy techniques), and physical property analysis method (electrical resistivity measurements) are proposed to study the phase transformation process of the alloy [5,6]. Although the microstructure analysis method and the physical property analysis method provide information in a straightforward way, they are heavy in workload and tedious in experimental operation, which means they are more suitable for verifying the results of phase transformation calculation. Therefore, thermal analysis method

**Corresponding author:** Pei FU, Tel: +86-15399211868, E-mail: [fupei\\_2015@csu.edu.cn](mailto:fupei_2015@csu.edu.cn);

Zhuo CHEN, Tel: +86-13974891750, E-mail: [chenzhuo@csu.edu.cn](mailto:chenzhuo@csu.edu.cn)

DOI: 10.1016/S1003-6326(22)65905-3

1003-6326/© 2022 The Nonferrous Metals Society of China. Published by Elsevier Ltd & Science Press

such as the cooling curve analysis (CCA), the differential scanning calorimetry (DSC), the differential thermal analysis (DTA) and the dilatometry analysis (DA) techniques are used more widely [7–10]. But to some extent, requirements for sample size and atmosphere in laboratory testing are high in the DSC, the DTA and the DA techniques [11]. Besides, the DTA method is applicable in the case that the cooling rate of sample is lower than 20 °C/min, which does not meet the requirement of the wide cooling rate range in the practical heat treatment process [12]. Although the DA techniques can be applied to a wider range of cooling rates, it is not suitable when the volume change of sample due to phase transformation is not obvious [13].

The CCA method, based on the cooling curve obtained in the cooling process, is less difficult in experiment and more flexible in mathematical analysis [14]. According to the number of required measuring points, two major CCA methods were proposed: the Fourier thermal analysis method and the Newtonian thermal analysis method [15–17]. For the Fourier thermal analysis method, the heat conduction behavior inside the sample is considered, which means the temperature distribution is non-uniform in the alloy sample. Thus, at least two measuring points in the one-dimensional temperature field are required to solve the temperature gradient. Besides, the change in specific heat capacity due to the phase transformation is taken into consideration [18]. Although this method has good accuracy and applicability, the high requirement for the number and position of thermocouples on the sample makes it difficult to obtain the necessary temperature data in the practical experiment.

Compared with the Fourier thermal analysis method, the alloy sample is regarded to be isothermal during the cooling process in the Newtonian thermal analysis method. So, only a single cooling curve measured in the experiment is required to calculate the released latent heat. The idea of the Newtonian thermal analysis method is to obtain the first derivative of the cooling curve with respect to time (FDC), and the zero curve (ZC) which is the first derivative of the reference curve without phase transformation. The product of the area enclosed by the two curves and the specific heat capacity is the phase transformation latent heat

released by the alloy sample during the cooling process. For the Newtonian thermal analysis method, the ZC is assumed through the temperature and time at the beginning and the end of the phase transformation on the cooling curve. The choice of the temperature and time affects the accuracy of the latent heat calculation results. The improved Newtonian thermal analysis method is proposed through determining the ZC by fitting the cooling curve before the phase transformation without fitting the temperature and time of the phase transformation [15].

As an advanced superalloy, the nickel-based superalloy has been widely used in the aircraft engine turbine disc component due to the excellent mechanical performance such as good corrosion resistance and oxidation resistance, and high strength [19–21]. However, there are few studies on the phase transformation of nickel-based superalloy and even less study on the latent heat release, mainly focusing on the measurement of phase transformation temperature range [22–24].

In this work, the Newtonian thermal analysis method and the improved Newtonian thermal analysis method are discussed based on the cooling curve, and the validity of two methods is present by calculating the phase transformation latent heat of 45<sup>#</sup> steel. Furthermore, the phase transformation latent heat of the self-designed CSU-A1 powder metallurgy nickel-based superalloy in the end-quench test is calculated, and the effect of cooling rate on latent heat release of phase transformation is analyzed. The study of the phase transformation latent heat will be helpful to the temperature and cooling rate control during the heat treatment process, optimizing the properties of the nickel-based superalloy.

## 2 Newtonian and improved Newtonian thermal analysis method

### 2.1 Newtonian thermal analysis method

Based on the cooling curve of the alloy sample, the following assumptions are made when applying the Newtonian thermal analysis method to calculate the latent heat of phase transformation:

- (1) The entire sample is regarded as a lumped parameter system;
- (2) During the cooling process, the density and specific heat capacity of the alloy sample remain

constant;

(3) Heat conduction is ignored inside the sample during the cooling process.

Based on the law of energy conservation, the phase transformation latent heat released inside the sample is equal to the sum of the thermodynamic internal energy of the sample and the heat released to the environment. It is described as follows:

$$\rho c \frac{dT}{dt} V = -hA(T - T_\infty) + \rho V L \frac{df}{dt} \quad (1)$$

As the density and specific heat capacity of the alloy sample are considered to be constant, the FDC is obtained by Eq. (1):

$$\left( \frac{dT}{dt} \right)_{\text{FDC}} = -\frac{hA}{\rho c V} (T - T_\infty) + \frac{L}{c} \frac{df}{dt} \quad (2)$$

where  $h$  is the surface heat transfer coefficient,  $W/(m^2 \cdot K)$ ;  $\rho$  is the density,  $kg/m^3$ ;  $c$  is the specific heat capacity,  $J/(kg \cdot K)$ ;  $T$  and  $T_\infty$  are the temperature of sample and the ambient temperature,  $^\circ C$ ;  $t$  is time, s.  $T$  changes with  $t$  during the cooling process.  $A$  is the heat transfer surface area between the sample and its surroundings,  $m^2$ ;  $V$  is the volume of sample,  $m^3$ .  $L$  ( $J/kg$ ) and  $f$  are the latent heat and volume fraction during the phase transformation.

Assuming that the phase transformation does not happen in the alloy sample during the cooling process, the ZC is calculated by the simplified mode of Eq. (2):

$$\left( \frac{dT}{dt} \right)_{\text{ZC}} = -\frac{hA}{\rho c V} (T - T_\infty) \quad (3)$$

Subtracting Eq. (3) from Eq. (2) yields

$$L \frac{df}{dt} = c \left[ \frac{dT}{dt} - \left( \frac{dT}{dt} \right)_{\text{ZC}} \right] \quad (4)$$

The latent heat release of phase transformation during the cooling process of the alloy sample can be obtained by integrating Eq. (4) as follows:

$$L \int_0^1 df = c \int_{t_i}^{t_f} \left[ \frac{dT}{dt} - \left( \frac{dT}{dt} \right)_{\text{ZC}} \right] dt \quad (5)$$

where  $t_i$  and  $t_f$  are the initial time and final time of the phase transformation in the alloy, s.

ZC is the key point to calculate the phase transformation latent heat. To determine the ZC, Eq. (3) is transformed to

$$\frac{dT}{T - T_\infty} = -\frac{hA}{\rho c V} dt \quad (6)$$

By introducing the excess temperature  $\theta = T - T_\infty$ , Eq. (6) can be further changed to

$$\frac{d\theta}{\theta} = -\frac{hA}{\rho c V} dt \quad (7)$$

Integrating Eq. (7) from 0 to  $t$  yields

$$\int_{\theta_0}^{\theta} \frac{d\theta}{\theta} = -\int_0^t \frac{hA}{\rho c V} dt \quad (8a)$$

$$\ln \frac{\theta}{\theta_0} = -\frac{hA}{\rho c V} t \quad (8b)$$

$$\frac{\theta}{\theta_0} = \frac{T - T_\infty}{T_0 - T_\infty} = \exp\left(-\frac{hA}{\rho c V} t\right) \quad (8c)$$

Equation (8c) can be transformed into

$$T = T_\infty + k_1 \cdot \exp(-k_2 t) \quad (9)$$

$$k_1 = T_0 - T_\infty, \quad k_2 = \frac{hA}{\rho c V}$$

where  $T_0$  is the initial temperature of the alloy sample,  $^\circ C$ .

Differentiating Eq. (9) yields

$$\left( \frac{dT}{dt} \right)_{\text{ZC}} = -k_1 \cdot k_2 \cdot \exp(-k_2 t) \quad (10)$$

It is illustrated that the ZC can be represented by an exponential function. The values of  $k_1$  and  $k_2$  are obtained by fitting the initial temperature and final temperature of the phase transformation on the cooling curve. The calculation accuracy of latent heat release is affected by the choice of the phase transformation time and temperature.

## 2.2 Improved Newtonian thermal analysis method

The main difference between the Newtonian thermal analysis method and the improved Newtonian thermal analysis method is the processing method of the ZC. The reference curve in the hypothetical cooling case when no phase transformation occurs is established in the improved Newtonian thermal analysis method.

There is an inflection point of temperature on the measured cooling curve due to the phase transformation during the cooling process. From the measured cooling curve before the inflection point, it is regarded that no phase transformation happens,

which is the basis for obtaining the reference curve.

In the improved Newtonian thermal analysis method, firstly, the cooling curve and the FDC are obtained in the same way as the Newtonian thermal analysis method. Then, the reference curve is obtained by fitting the section of cooling curve before phase transformation. The ZC is obtained by taking the derivative of the fitting function as follows:

$$\left(\frac{dT}{dt}\right)_{ZC} = f'_r(t) \quad (11)$$

where  $f_r(t)$  is the fitting reference curve. ZC is generally exponential or nearly linear function of time.

Finally, by combining Eq. (11) with Eq. (5), the phase transformation latent heat during the cooling process of the alloy sample can be obtained. The initial time and final time of the phase transformation in the alloy are determined by the intersection of the FDC and ZC.

### 3 Model verification of Newtonian and improved Newtonian thermal analysis method

There is limited research on the phase transformation and corresponding physical parameters of the self-designed CSU-A1 powder metallurgy nickel-based superalloy. However, the phase transformation kinetics model and physical parameter of 45<sup>#</sup> steel are widely studied [25,26]. Therefore, the phase transformation latent heat of 45<sup>#</sup> steel is calculated to verify the validity of the Newtonian thermal analysis method and the improved Newtonian thermal analysis method.

#### 3.1 Cooling curve of 45<sup>#</sup> steel

Due to the limited temperature measuring point in the practical experiment, the end-quench test of 45<sup>#</sup> steel is numerically simulated by DEFORM software to obtain the cooling curve with high efficiency and low cost. The chemical composition of 45<sup>#</sup> steel is listed in Table 1.

**Table 1** Chemical composition of 45<sup>#</sup> steel (wt.%)

C	Si	Mn	Cu	
0.42–0.45	0.17–0.37	0.5–0.8	≤0.25	
Ni	Cr	P	S	Fe
≤0.25	≤0.25	≤0.035	≤0.035	Bal.

The sample of 45<sup>#</sup> steel was set as a cylinder of  $d25\text{ mm} \times 120\text{ mm}$  to be consistent with the practical end-quench test of CSU-A1 nickel-based superalloy. The thermal boundary conditions at the side and top of the sample are adiabatic, while the heat transfer coefficient is  $10\text{ W}/(\text{m}^2 \cdot ^\circ\text{C})$  at bottom to ensure that the sample is cooled slowly and thus the phase transformation latent heat can be fully released. During the cooling process, only the phase transformation from austenite to pearlite phase which happens between  $900$  and  $600\text{ }^\circ\text{C}$  is considered in order to simplify the phase transformation process of 45<sup>#</sup> steel. Therefore, the initial temperature of the sample is set at  $900\text{ }^\circ\text{C}$ . The physical parameters of austenite and pearlite phase of 45<sup>#</sup> steel are listed in Table 2.

**Table 2** Physical parameters of austenite and pearlite phase of 45<sup>#</sup> steel

Phase	Specific heat capacity/ ( $\text{J} \cdot \text{kg}^{-1} \cdot ^\circ\text{C}^{-1}$ )	Thermal conductivity/ ( $\text{W} \cdot \text{m}^{-1} \cdot ^\circ\text{C}^{-1}$ )	Density/ ( $\text{kg} \cdot \text{m}^{-3}$ )
Austenite	589.94	25.96	$7.85 \times 10^3$
Pearlite	741.53	32.85	$7.85 \times 10^3$

Combined with the phase transformation kinetics model of 45<sup>#</sup> steel in the built-in database of DEFORM, the unsteady solid heat transfer with phase transformation inside the sample during the end-quench test is studied, and thus the cooling curves with phase transformation latent heat at any position of the sample are obtained. The cooling curve at 50 mm away from bottom of the sample is selected to study the phase transformation latent heat of 45<sup>#</sup> steel, as shown in Fig. 1. The obvious

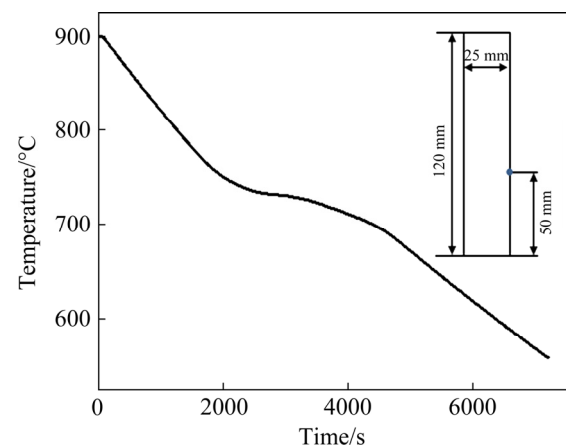


**Fig. 1** Cooling curve of measured point on test sample of 45<sup>#</sup> steel

temperature inflection point on the cooling curve illustrates that the phase transformation latent heat of 45<sup>#</sup> steel has a great influence on the temperature field during the cooling process.

### 3.2 Calculation and comparison of phase transformation latent heat of 45<sup>#</sup> steel

The generation of phase transformation is judged by the difference between the cooling curve and the reference cooling curve in the SS-DTA method, in which the reference cooling curve is obtained by piecewise linear fitting of the cooling curve as follows:

$$\Delta T(t) = T(t) - T_r(t) \quad (12a)$$

$$T_{ri}(t) = \begin{cases} m_i t + b_i, & l_i \leq t \leq l_{i+1} \\ 0, & \text{otherwise} \end{cases} \quad (12b)$$

where  $T(t)$  and  $T_r(t)$  are the temperatures on the cooling curve and the reference cooling curve, respectively.  $\Delta T(t)$  is the temperature difference, which can be used as the criterion for the generation of phase transformation when there is obvious fluctuation.  $m_i$  and  $b_i$  are the slope and intercept of each interval, and  $l_i$  is the cut-off point of each interval.

Based on the cooling curve obtained by numerical simulation, the initial temperature and final temperature of phase transformation are 759 and 746 °C obtained through the SS-DTA method and MATLAB code. The corresponding initial time and final time are 1837 and 2150 s through the Newtonian thermal analysis method, while the initial time and final time are 1368 and 4618 s through the improved Newtonian thermal analysis method. Therefore, the fitting values of  $k_1$  and  $k_2$  of ZC in Eq. (10) in the Newtonian thermal analysis method are 477.48 and 0.000111, respectively. The cooling curves, the FDCs and the ZCs of two methods are shown in Fig. 2.

Based on the FDCs, the ZCs and Eq. (5), the phase transformation latent heat of the 45<sup>#</sup> steel is calculated through the two methods. The results are compared with the phase transformation latent heat in literature [25] as given in Table 3.

Compared with the Newtonian thermal analysis method, the relative error of phase transformation latent heat through the improved Newtonian thermal analysis method is much smaller. This is because the ZC in the Newtonian

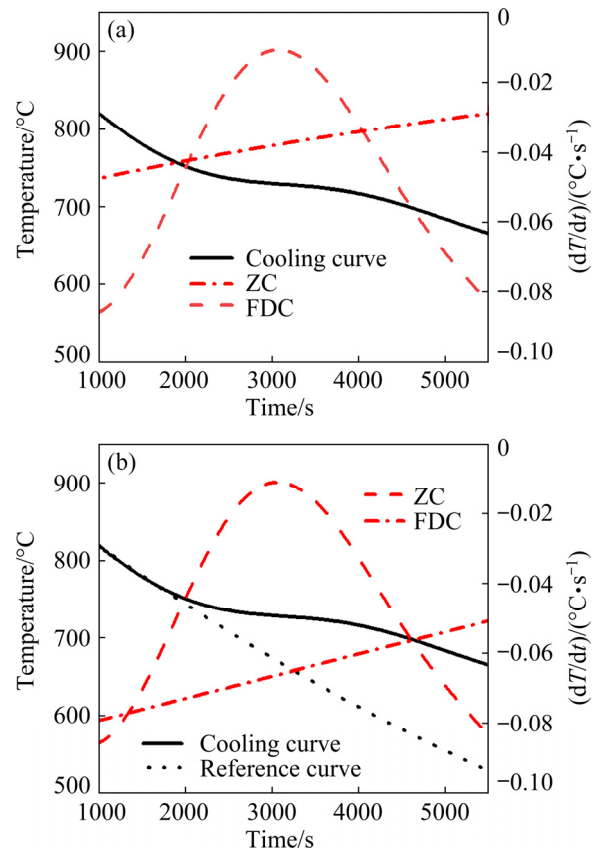


**Fig. 2** Curves with different methods of 45<sup>#</sup> steel: (a) Newtonian thermal analysis method; (b) Improved Newtonian thermal analysis method

**Table 3** Comparison of results of latent heat of phase transformation

Method	Latent heat/(J·g <sup>-1</sup> )	Relative error/%
Newtonian thermal analysis	40	48.39
Improved Newtonian thermal analysis	73.45	5.20
Literature data	77.5	—

thermal analysis method is obtained by fitting the initial temperature and time as well as final temperature and time of phase transformation based on the cooling curve. It is difficult to calculate the theoretical phase transformation time and temperature of alloy, especially the advanced super-alloy with complex composition. Experimental method such as SS-DTA method is generally used to determine the phase transformation time and temperature, which leads to inevitable error in the Newtonian thermal analysis method.

## 4 Calculation of phase transformation latent heat in nickel-based superalloy

### 4.1 End-quench test of CSU-A1 nickel-based superalloy

In the end-quench test, the cylindrical sample is heated over the solution temperature and then cooled by projecting cooling medium against the bottom. Therefore, the temperature and cooling rate distribute in gradient along the length of sample, corresponding to different properties [27–29]. The heating and end-quench experiment platform in the end-quench test with air of CSU-A1 nickel-based superalloy sample is shown in Fig. 3 [30]. With reference to the end-quench test standard (ISO 642—1999) [31], the cylinder sample has dimensions of  $d25\text{ mm} \times 120\text{ mm}$ , as shown in Fig. 4. Three S-type thermocouples at the distance of 5, 50 and 80 mm from bottom of the sample were arranged to record the temperature during the cooling process.

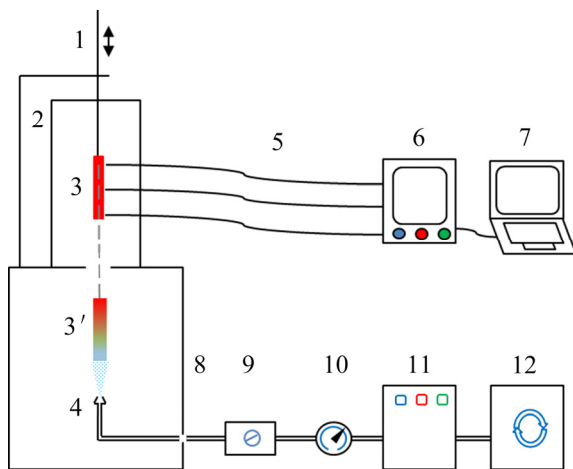


**Fig. 3** Schematic of end-quench test system: 1–Drive rod; 2–Resistance-heated furnace; 3–Heated sample; 3′–Cooled sample; 4–Nozzle; 5–S-type thermocouple; 6–Data acquisition device; 7–Control terminal; 8–Cooling box; 9–Flow controller; 10–Stabilizing valve; 11–Drying machine; 12–Air compressor

The sample was made of self-designed CSU-A1 powder nickel-based superalloy, which was manufactured by the rotating electrode comminuting process, hot isostatic pressing (HIP), and hot extrusion (HEX) in sequence. The chemical composition of the CSU-A1 nickel-based superalloy is illustrated in Table 4.

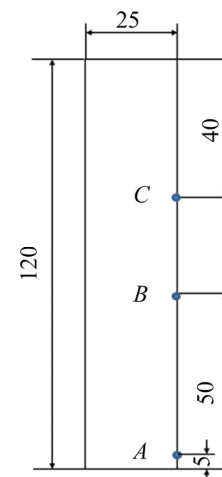


**Fig. 4** Schematic of test sample (unit: mm)

**Table 4** Chemical composition of CSU-A1 powder metallurgy nickel-based superalloy (wt.%)

Co	Cr	Mo	W	Al	Ti	Nb	C	Hf	Ni
26.1	13.5	4	3.9	3.3	26.1	13.5	0.05	0.2	Bal.

### 4.2 Cooling curve and average cooling rate of CSU-A1 nickel-based superalloy

The temperature curves at Points A, B and C (5, 50 and 80 mm away from the bottom) of the self-designed CSU-A1 powder metallurgy nickel-based superalloy sample measured in the same experiment are shown in Fig. 5.

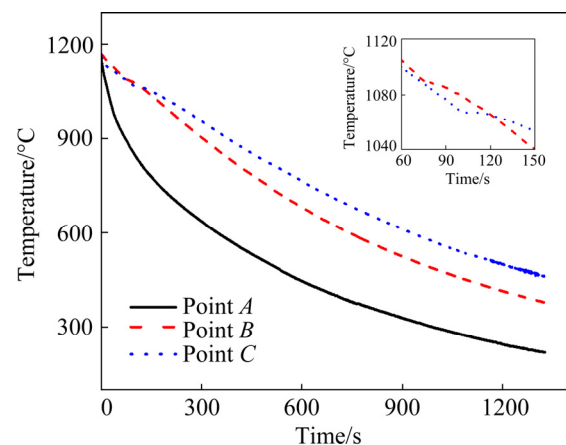


**Fig. 5** Cooling curves of CSU-A1 nickel-based superalloy in end-quench test

On the cooling curve at 50 and 80 mm, the decreasing trend of temperature is more moderate than that if no phase transformation occurs. The obvious temperature inflection point on the cooling curve illustrates that the temperature field during

the cooling process is affected by the latent heat release of phase transformation. However, the cooling curve at 5 mm is quite smooth because it cools too fast for the phase transformation latent heat to be released. The temperature at 5 mm drops faster than that at other positions because the heat transfer coefficient is much larger at bottom due to the intense impinging jet convection heat transfer.

The accuracy of S-type thermocouple is  $(2\pm 0.15\%)$  °C, and the temperature range in the end-quench test is 200–1150 °C, so the maximum relative error of temperature is  $\pm 1.86\%$ . Besides, the location of the thermocouple influences the accuracy of the temperature measured in the experiment. During the cooling process, due to the limited heat transfer rate, the temperature is different inside and outside the sample at the same cross section. In the experiment, the S-type thermocouples were weld on the outside surface of the sample, so the temperature measurement may be affected by the cooling medium. The accuracy of measured temperature may be improved by drilling holes and putting the thermocouples inside the sample, but the difficulty and cost of such approach will increase dramatically.

The average cooling rate of the nickel-based superalloy is defined as [2]

$$R_c = \frac{\Delta T}{\Delta t} = \frac{T_i - T_f}{\Delta t} \quad (13)$$

where  $T_i$  and  $T_f$  are the initial temperature and final temperature of phase transformation (the  $\gamma'$  phase precipitation) in the self-designed CSU-A1 powder nickel-based superalloy, respectively.  $\Delta T$  is the temperature difference between  $T_i$  and  $T_f$ , and  $\Delta t$  is the duration of the precipitation process.

Based on Eq. (13), the cooling rates of Points *A*, *B* and *C* in the end-quench test are calculated and given in Table 5.

**Table 5** Cooling rates of different measuring points

Measuring point	Cooling rate/(°C·min <sup>-1</sup> )
<i>A</i>	194.69
<i>B</i>	50.15
<i>C</i>	40.06

The cooling rate at Point *A* is much larger than that at Point *B* and Point *C*, which illustrates that the cooling rate decreases significantly when the distance from the quenched end of the sample

increases. This is because, in addition to the radiation heat transfer, the forced convection caused by impinging jets at the quenched end is the main heat transfer mode of the sample. The temperature near the bottom of the sample drops more quickly than that near the top due to the larger heat transfer coefficient at the quenched end, so the cooling rate near the bottom is much larger.

### 4.3 Phase transformation latent heat of CSU-A1 nickel-based superalloy

When considering the experiment in practice, there may be no obvious temperature inflection point caused by phase transformation on the measured cooling curve when the cooling rate is too large. Besides, the thermocouple on the side surface of the alloy sample is easy to fall off because of high temperature. Thus, cooling curves with different cooling rates from several experiments are used to analyze the latent heat release of the self-designed CSU-A1 powder metallurgy nickel-based superalloy. Four cooling curves and corresponding FDCs, reference curves and ZCs of the CSU-A1 nickel-based superalloy are shown in Fig. 6.

Based on the FDCs and the ZCs, the latent heat release of phase transformation of the self-designed CSU-A1 powder metallurgy nickel-based superalloy with different cooling rates is calculated by the improved Newtonian thermal analysis method. The latent heat release with corresponding cooling rate is given in Table 6.

As the cooling rate decreases, the latent heat release of phase transformation of the self-designed CSU-A1 powder metallurgy nickel-based superalloy increases. When the cooling rate is small, there is enough time for the alloy microstructure to go through the phase transformation process of nucleation, growth, and coarsening. So, with smaller cooling rate, the phase transformation process of the self-designed CSU-A1 powder metallurgy nickel-based superalloy is completed more fully and more latent heat is released. Generally, the latent heat release of phase transformation remains a constant when the cooling rate decreases to a critical value because the latent heat is released completely. Similarly, the latent heat of phase transformation will decrease to zero when the cooling rate increases to a critical value because there is no time for the latent heat to be released.

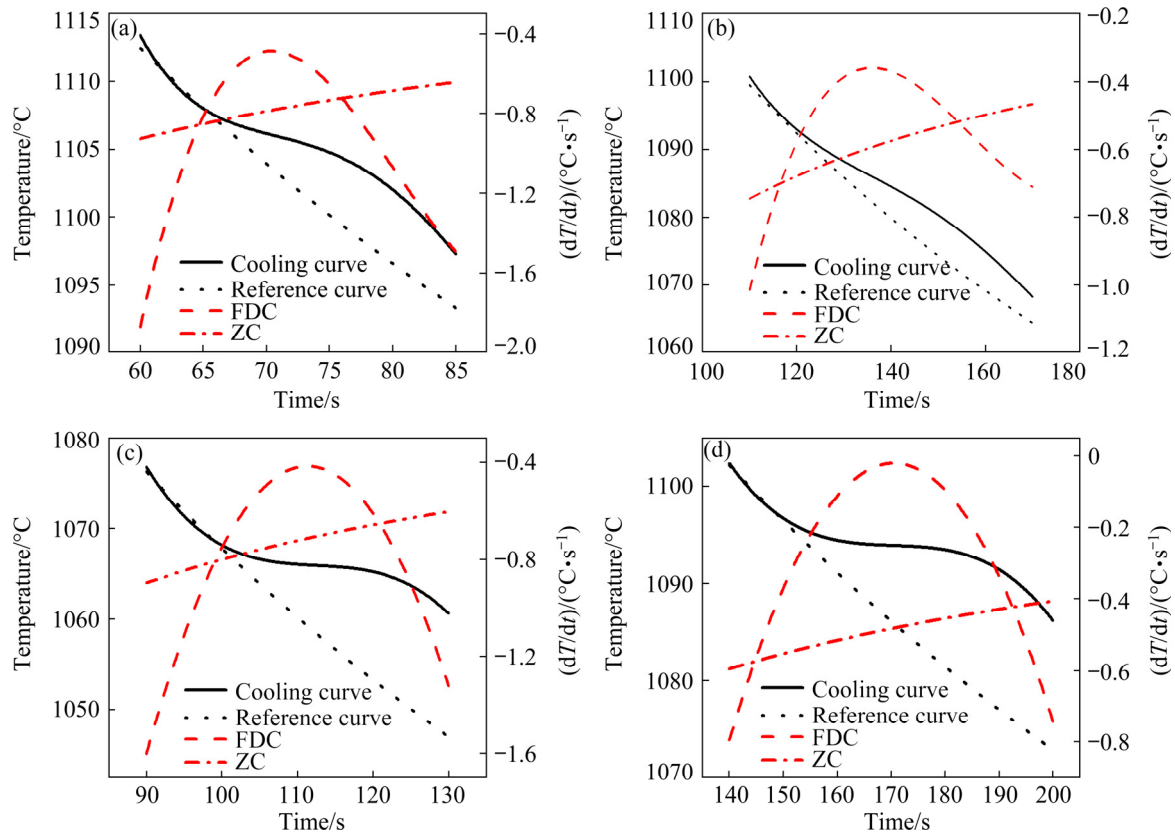


**Fig. 6** Curves with different cooling rates of CSU-A1 nickel-based superalloy: (a) 50.15 °C/min; (b) 44.00 °C/min; (c) 40.06 °C/min; (d) 33.40 °C/min

**Table 6** Relationship between cooling rate and latent heat release of phase transformation

Cooling rate/(°C·min <sup>-1</sup> )	Latent heat/(J·g <sup>-1</sup> )
50.15	4.3
44.00	4.69
40.06	9.86
33.40	12.29

## 5 Conclusions

(1) The Newtonian thermal analysis method and the improved Newtonian thermal analysis method were proposed to study the phase transformation latent heat based on the cooling curve. The validity of two methods is given by the phase transformation latent heat of 45<sup>#</sup> steel. The relative error of the Newtonian thermal analysis method is 48.39%, while relative error of the improved Newtonian thermal analysis method is 5.20%. The improved Newtonian thermal analysis method can effectively improve the calculation accuracy of phase transformation latent heat.

(2) End-quench test system was established to

study the cooling process of the self-designed CSU-A1 powder metallurgy nickel-based superalloy. S-type thermocouples at different positions of the sample were arranged to record the temperature during the cooling process to provide the necessary data for the phase transformation study.

(3) The cooling rate affects the release of phase transformation latent heat of the self-designed CSU-A1 powder metallurgy nickel-based superalloy. When the cooling rate decreases from 50.15 to 33.40 °C/min, the latent heat release of phase transformation increases from 4.3 to 12.29 J/g. As the cooling rate decreases, the latent heat release of phase transformation will increase due to sufficient time for the alloy microstructure to complete the phase transformation process.

## Acknowledgments

We appreciate the financial supports from the National Key Research and Development Program of China (No. 2016YFB0700300), and the Postgraduate Independent Exploration and Innovation Project of Central South University, China (No. 2019zzts262).

## References

- [1] FU Tian-liang, WANG Zheng-dong, LI Yong, LI Jia-dong, WANG Guo-dong. The influential factor studies on the cooling rate of roller quenching for ultra heavy plate [J]. *Applied Thermal Engineering*, 2014, 70(1): 800–807.
- [2] WU Hong-yu, LI Jia, LIU Feng, HUANG Lan, ZENG Xin, FANG Hong-qi, HUANG Zai-wang, JIANG Liang. A high-throughput methodology search for the optimum cooling rate in an advanced polycrystalline nickel-based superalloy [J]. *Materials & Design*, 2017, 128: 176–181.
- [3] YAZDI A Z, SAJJADI S A, ZEBARJAD S M, NEZHAD S M M. Prediction of hardness at different points of Jominy specimen using quench factor analysis method [J]. *Journal of Materials Processing Tech*, 2008, 199(1/2/3): 124–129.
- [4] WEI He, CHEN Yin-li, SU Lan, DI Tang. Effect of cooling rate and isothermal temperature on the phase transformation and microstructure evolution in SWRH82B high-carbon steel [J]. *Materials Research Express*, 2018, 5: 086506.
- [5] ZHAO Nai-qin. Solid-state phase transformation of alloys [M]. Changsha: Central South University Press, 2008. (in Chinese)
- [6] BENRABAH I E, ALTINKURT G, FEVRE M, DEHMAS M, DENAND B, FOSSARD F, MEROT J S, GEANDIER G, LOCQ D, PERRUT M. Monitoring the kinetics of the  $\gamma'$  phase in the N18 superalloy using in situ electrical resistivity measurements [J]. *Journal of Alloys and Compounds*, 2020, 825: 154108.
- [7] ALEXANDROV B T, LIPPOLD J C. Single sensor differential thermal analysis of phase transformations and structural changes during welding and postweld heat treatment [J]. *Welding in the World*, 2007, 51(11/12): 48–59.
- [8] BADJI R, KHERROUBA N, MEHDI B, CHENITI B, BOUABDALLAH M, KAHLOUN C, BACROIX B. Precipitation kinetics and mechanical behavior in a solution treated and aged dual phase stainless steel [J]. *Materials Chemistry & Physics*, 2014, 148(3): 664–672.
- [9] ALEXANDROV B, LIPPOLD J, TATMAN J, MURRAY G. Non-equilibrium phase transformation diagrams in engineering alloys [C]//Trends in Welding Research, Proceedings of the 8th International Conference. 2009: 467–476.
- [10] GIBBS J W, SCHLACHER C, KAMYABI-GOL A, MAYR P, MENDEZ P F. Cooling curve analysis as an alternative to dilatometry in continuous cooling transformations [J]. *Metallurgical and Materials Transactions A*, 2015, 1: 1–8.
- [11] TANG Peng, HU Zhi-liu, ZHAO Yan-jun, HUANG Qing-bao. Investigation on the solidification course of Al–Si alloys by using a numerical Newtonian thermal analysis method [J]. *Materials Research Express*, 2017, 4(12): 126511.
- [12] GIBBS J W, MENDEZ P F. Solid fraction measurement using equation-based cooling curve analysis [J]. *Scripta Materialia*, 2008, 58(8): 699–702.
- [13] LUO Si-hua, HUANG Zai-wang, XIE Zi-wei, ZHOU Ping, JIANG Liang. High-throughput characterization phase transformation temperature based on end-quenching methodology [J]. *Materials Research Express*, 2018, 6(3): 36503–36503.
- [14] STEFANESCU D M. Thermal analysis—Theory and applications in metal casting [J]. *International Journal of Metalcasting*, 2015, 1(9): 7–22.
- [15] BARLOW J O, STEFANESCU D M. Computer-aided cooling curve analysis re-visited [M]. Philadelphia: Transactions of the American Foundry Society, 1997.
- [16] KAPTURKIEWICZ W, BURBIELKO A, LOPEZ H F. A new concept in thermal analysis of castings [J]. *American Foundry Society*, 1993, 1: 505–511.
- [17] DIOSZEGI A, HATTEL J H. Inverse thermal analysis method to study solidification in cast iron [J]. *International Journal of Cast Metals Research*, 2004, 17(5): 311–318.
- [18] SVIDRO J T, DIOSZEGI A, TOTTH J. The novel application of Fourier thermal analysis in foundry technologies [J]. *Journal of Thermal Analysis & Calorimetry*, 2014, 115(1): 331–338.
- [19] POLLOCK, TRESA M. Alloy design for aircraft engines [J]. *Nature Materials*, 2016, 15(8): 809–815.
- [20] SINGHA A R P, NAG S, HWANGA J Y, VISWANATHANB G B, TILEY J, SRINIVASAND R, FRASER H L, BANERJEE R. Influence of cooling rate on the development of multiple generations of  $\gamma'$  precipitates in a commercial nickel base superalloy [J]. *Materials Characterization*, 2011, 62: 878–886.
- [21] FURRER D U, SHANKAR R, WHITE C. Optimizing the heat treatment of Ni-based superalloy turbine discs [J]. *JOM*, 2003, 55(3): 32–34.
- [22] FUCHS G E, BOUTWELL B A. Modeling of the partitioning and phase transformation temperatures of an as-cast third generation single crystal Ni-base superalloy [J]. *Materials Science and Engineering A*, 2002, 333: 72–79.
- [23] RUAN J J, UESHIMA N, OIKAWA K. Phase transformations and grain growth behaviors in superalloy 718 [J]. *Journal of Alloys and Compounds*, 2018, 737: 83–91.
- [24] ZHENG Liang, LIU Yu-feng, GORLEY M J, HONG Zu-liang, DAY S, TANG C C, LI Zhou, XIAO Cheng-bo, ZHANG Guo-qing. The DSC investigation on phase transformations of directionally solidified (DS) and powder metallurgy (PM) Ni-base superalloys [J]. *Materials Science Forum*, 2018, 941: 1035–1040.
- [25] LEE S J, PAVLINA E J, CHESTER J, TYNE C J V. Kinetics modeling of austenite decomposition for an end-quenched 1045 steel [J]. *Materials Science and Engineering A*, 2010, 527: 3186–3194.
- [26] NUNURA C R N, SANTOS C A D, SPIM J A. Numerical-experimental correlation of microstructures, cooling rates and mechanical properties of AISI 1045 steel during the Jominy end-quench test [J]. *Materials & Design*, 2015, 76: 230–243.
- [27] JOMINY W E, BOEGEHOLD A L. A hardenability of steel [J]. *Transactions of ASM*, 1938, 26: 574–606.
- [28] FU Pei, ZHOU Ping, XIE Zi-wei, WU Hong-yu, CHEN Ji-guang. Experimental and CFD investigations on cooling process of end-quench test [J]. *Transactions of Nonferrous Metals Society of China*, 2019, 29: 2440–2446.
- [29] WU Hong-yu, HUANG Zai-wang, ZHOU Ning, CHEN

- Ji-guang, ZHOU Ping, JIANG Liang. A study of solution cooling rate on  $\gamma'$  precipitate and hardness of a polycrystalline Ni-based superalloy using a high-throughput methodology [J]. Materials Science and Engineering A, 2019, 739: 473–479.
- [30] FU Pei, ZHOU Ping, ZHAO Tian-yang, SONG Yan-po, HUANG Zai-wang. Study of the heat transfer coefficient of a nickel-based superalloy in the end-quench test with air [J]. International Journal of Thermal Sciences, 2020, 155: 106416.
- [31] ISO 642—1999. Steel hardenability test by end quenching (Jominy test) [S]. British: European Committee for Standardization, 1999.

## 基于端淬实验冷却曲线的相变潜热计算及其在镍基高温合金中的应用

赵天阳<sup>1</sup>, 付佩<sup>1</sup>, 陈卓<sup>1</sup>, 周萍<sup>1</sup>, 李超<sup>2</sup>

1. 中南大学 能源科学与工程学院, 长沙 410083;
2. 中南大学 粉末冶金国家重点实验室, 长沙 410083

**摘要:** 为了高效、低成本获取合金在不同冷却速率下的相变潜热, 讨论基于端淬实验冷却曲线的牛顿热分析方法和改进牛顿热分析方法。通过对 45# 钢相变潜热的计算验证这两种方法的有效性。结果表明, 改进的牛顿热分析方法得到的相变潜热相对误差为 5.20%, 比牛顿热分析方法更准确。当冷却速率从 50.15 °C/min 降低到 33.40 °C/min 时, 自制的 CSU-A1 粉末冶金镍基高温合金相变潜热释放量从 4.3 J/g 增加到 12.29 J/g, 这是因为当冷却速度较小时, 合金组织有足够的时间完成相变过程。

**关键词:** 冷却曲线; 端淬实验; 牛顿热分析方法; 相变潜热; 镍基高温合金

(Edited by Bing YANG)